

V. PAVLIKOV¹, K. BELOUSOV², S. ZHYLA¹, E. TSERNE¹,
 O. SHMATKO¹, A. SOBKOLOV¹, D. VLASENKO¹, V. KOSHARSKYI¹,
 O. ODOKIENKO¹, M. RUZHENTSEV¹

¹ National Aerospace University “Kharkiv Aviation Institute”, Ukraine

² Measuring Systems and Telecommunications in Yuzhnoye SDO, Dnipro, Ukraine

RADAR IMAGING COMPLEX WITH SAR AND ASR FOR AEROSPACE VEHICLE

The subject of study in the article is the algorithms for radio monitoring of the Earth in a wide field of view from aerospace transport. The goal is to design a structural diagram of a radio complex that can operate simultaneously in two modes: modified synthetic aperture (SAR) and aperture synthesis (ASR), in accordance with algorithms synthesized by the maximum likelihood method. The modified SAR mode allows obtaining high-resolution radio images in the observation angle range $\pm(20^\circ...50^\circ)$ from the direction to the nadir. A method of combining a modified SAR algorithm is used, which differs from the classical imaging algorithm by the possibility of obtaining a higher spatial resolution, the payment for this is the complication of the signal processing algorithm associated with the implementation of decorrelating filters that expand the spectrum of received signals in each receiving path, and the ASR mode, which allows imaging using passive or active radar principles. The passive ASR mode provides for the imaging in the observation angle range of $\pm 20^\circ$ from the nadir based on the results of processing signals of its own broadband radio-thermal radiation, and the active mode – in the same observation angle range, but using the broadband noise signal of the backlight. An important result in the formation of a radio image in the specified viewing area when using the active mode of the ASR is that the images are close in physical content, namely, proportional to the specific effective reflection surface of the underlying surface. In addition, a distinctive feature of the synthesized algorithms is the use of wideband probing signals and, accordingly, the same input paths of receivers, which makes it possible to increase the signal-to-noise ratio of the output effect. Conclusions. The scientific novelty of the results obtained is as follows: a structural diagram of the radio complex was developed on the basis of algorithms synthesized by the maximum likelihood method. For the formation of a radio image in the radio complex, a combination of SAR and ASR (with two modes of operation) is implemented. This implementation is important, since it allows obtaining high-resolution images in the observation angle range of $\pm 50^\circ$ from the direction to the nadir. It is advisable to place the complex on airplanes, helicopters and spacecraft (preferably those that move in low orbits).

Keywords: radar imaging; synthetic aperture radar; aperture synthesis radar; signal processing algorithm; ultrawideband signal processing.

Introduction

Motivation. High information content about the Earth's surface can be obtained using optical and radar surveys [1, 2] from an aerospace carrier. At the same time, radar images are much more informative in conditions of limited optical visibility due to cloudiness, smoke, darkness, etc. This creates the preconditions for the widespread use of aerospace-based radars capable of imaging. However, it should be noted that to ensure high spatial resolution (comparable to the resolution of images in the optical range), it is necessary to develop and implement complex algorithms for processing radio signals [3 - 7], as well as algorithms for their filtering [8, 9]. In particular, filtering algorithms are necessary because radio images obtained by active radars are usually distorted by a high level of speckle-noise.

Today, two main signal processing algorithms are used to ensure high spatial resolution of radar images.

These are synthesis of antenna aperture algorithm implemented by synthetic aperture radar systems (SAR) [10, 11], and an aperture synthesis algorithm implemented in passive aperture synthesis radar (ASR) [12-14]. Each has its own advantages and disadvantages. Thus, SAR allows obtaining high spatial resolution of the image in the range of observation angles $\pm(20^\circ...50^\circ)$ from the direction to the nadir [15-17], but does not provide a high resolution in the range of $\pm 20^\circ$ from the nadir. ASR, on the other hand, allows us to get an image in the range of $\pm 20^\circ$ from the nadir. Therefore, as shown in [18, 19], it is advisable to combine these radio systems into a single complex capable of forming radar images in a swath of $\pm 50^\circ$ from nadir.

State of the Art. It should be noted that significant advances in the field of increasing the spatial resolution of images are obtained due to the ability to form and process wide- and ultra-wideband signals [20-22]. The

modern radioelement base makes it possible to design ultra-wideband radars. Such radars can be multi-position [23, 24], single-position with probing through obstacles [25-27], single-position but with multi-frequency signal processing [28], single-position with very short pulse signals [29]. Unlike all of the above, the designed complex is supposed to work not with ultra-short pulse signals, but with ultra-wideband noise signals [20-22]. The latter is very important for meeting the modern requirements of Green Engineering [30].

Objectives. The report develops the works [3, 15-19, 31] and proposes the synthesis of a radio complex with the processing of wideband spatio-temporal signals to obtain radar images in the range of observation angles $\pm 50^\circ$ from nadir with high spatial resolution.

Purpose of the article: designing and research an aerospace-based radio complex capable of forming high spatial resolution radio images in the sector of observation angles $\pm 50^\circ$.

Radar Imaging Algorithms

A. Modified SAR Imaging Algorithm

We will solve the problem of synthesizing a signal processing algorithm for forming images in the field of view $\pm(20^\circ \dots 50^\circ)$ from the nadir. For this, we will use a unified recording [32-34] of a set of wideband probing signals

$$s(t) = \operatorname{Re} \exp(-j\varphi_0) \times \sum_{n=1}^N \dot{B}_n(t) \exp(j2\pi f_0(t - (n-1)T_r)), \quad (1)$$

where $\dot{B}_n(t)$ is the complex envelope of the n -th pulse ($n = 1..N$) in the set, which, for example, can describe linear frequency modulation (Chirp) $\dot{B}_n(t) = \Pi(t - (n-1)T_r) \exp(j\pi\Delta F T^{-1}(t - (n-1)T_r)^2)$;

$\Pi(t - (n-1)T_r)$ is the radio pulse envelope;

ΔF is the bandwidth;

T is the signal duration;

T_r is the pulse repetition period in the set;

f_0 is the central frequency of the emitted signal;

t is the time;

φ_0 is the initial phase;

j is the complex unit.

The expression for $\dot{B}_n(t)$ can have other forms of notation [35, 36], which does not significantly affect the physical properties of the chirp signal.

We will specify the width of the passband ΔF during the simulation; we only note that it must satisfy

the wideband condition [37-39]. It should be noted that today there are several options for defining the concept of broadband (at different levels of spectrum falloff from its maximum value) [40-42] and ultra-wideband (in the context of using ultrashort pulses) [43, 44] signals. The choice of a specific criterion of broadband is advisable to carry out based on the specific task under consideration. In fig. 1 it is shown the geometry of the problem, which is necessary for solving the problems of synthesis of signal processing algorithms.

In fig. 1 introduced the following designations: V is the flight speed; t is the time; t_0 is the beginning of synthesis; $R(t, \cdot)$, $R_p(t, \cdot)$ are the current distances from the phase center of the transmitting antenna to the element of the underlying surface and from this element to the p -th element of the antenna system ($p = 1..Q$); A_p are the elements of the receiving antenna; A_{tr} is the transmitter antenna; \mathbf{r} is the radius vector from the projection of the phase center of the transmitting antenna on the underlying surface to the elementary area D with coordinates (x_C, y_C) ; h is the flight altitude of the aircraft.

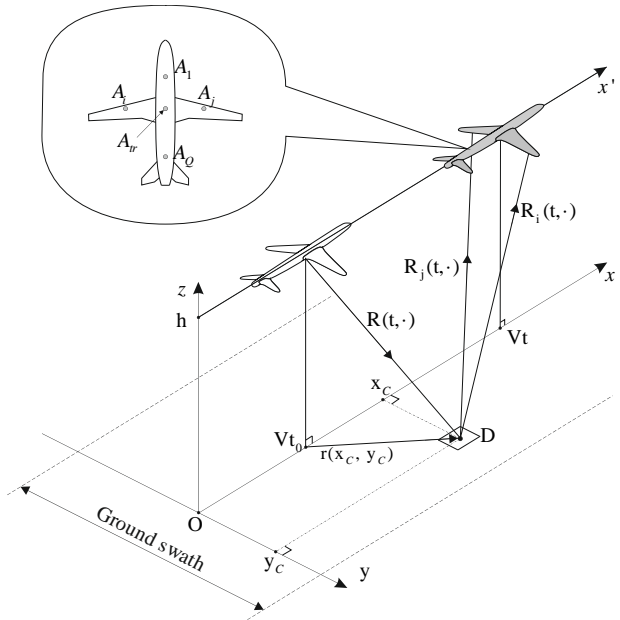


Fig. 1. Geometry of the radar imaging problem

The signal reflected by a single element of the underlying surface, the coordinates of which are determined by a vector \vec{r} (Fig. 1), can be written in the following form

$$\begin{aligned} s_s(t, h, r) = & G_{tr}(t - t_d(h, r)) \exp(-j\varphi_0) \times \\ & \times \sum_{n=1}^N \dot{B}_n(t - t_d(h, r)) \times \\ & \times \exp(j2\pi f_0(t - (n-1)T_r - t_d(h, r))), \end{aligned} \quad (2)$$

where h is the flight altitude of the aerospace carrier; $t_d(h, \mathbf{r})$ is the signal propagation delay time;

$\dot{G}_{tr}(t - t_d(h, \mathbf{r}))$ is the complex radiation pattern of the transmitting antenna in the direction of the surface with coordinates \mathbf{r} .

The signal reflected within the irradiation zone of the underlying surface, which entered the receiving antenna, can be written as follows

$$\dot{s}(t) = \exp(j\varphi) \int_D \dot{G}_r(t, \mathbf{r}) \dot{F}(\mathbf{r}) \dot{s}_s(t, h, \mathbf{r}) d\mathbf{r}, \quad (3)$$

where $\dot{F}(\mathbf{r})$ is the specific complex reflection coefficient of the underlying surface element with coordinates \mathbf{r} ;

$\dot{G}_r(t, \mathbf{r})$ is the complex radiation pattern of the receiving antenna in the direction of the underlying surface element with coordinates \mathbf{r} (limits the irradiation zone of the underlying surface).

Phase φ uncontrollable, but it can be neglected in coherent signal processing.

We can write the observation equation in the form of an additive mixture of signal (3) and noise

$$u(t) = \text{Re}\{\dot{s}(t)\} + n(t), \quad (4)$$

where $n(t)$ is the internal noise of the receiver (white Gaussian noise with zero mean).

The signal processing algorithm in the modified SAR (MSAR) is found by the maximum likelihood method [45] from the solution of the likelihood equation with respect to the optimal recovery of the specific effective reflection surface of the surface elements $\sigma(\mathbf{r})$, which can be considered as a radar image,

$$\frac{\delta \ln p(u(t) | \sigma(\mathbf{r}))}{\delta \sigma(\mathbf{r}')} = \frac{\delta}{\delta \sigma(\mathbf{r}')} \ln \left\{ k(\sigma(\mathbf{r})) \times \right. \\ \left. \times \exp \left(-\frac{1}{2} \int_0^T \int_0^T u(t_1) W(t_1, t_2, \sigma(\mathbf{r})) u(t_2) dt_1 dt_2 \right) \right\} = 0, \quad (5)$$

where $\frac{\delta}{\delta \sigma(\mathbf{r}')}$ is the variational derivative of the specific effective reflection surface of the underlying surface;

$W(t_1, t_2, \sigma(\mathbf{r}))$ is the inverse function to the correlation function of the observation equation.

Solution (5) can be reduced to the following algorithm for optimal signal processing in MSAR (the transition to complex envelope processing is taken into account):

$$\hat{I}_{MSAR}(\mathbf{r}) = \int_0^T \int_0^T \dot{U}(t_1) W(t_1, t_2, \sigma(\mathbf{r})) \dot{S}_s^*(t_2, h, \mathbf{r}) dt_1 dt_2,$$

where $\dot{U}(t_1)$ is the complex observation envelope;

$\dot{S}_s^*(t_2, h, \mathbf{r})$ is the complex conjugate complex envelope of the signal (2).

The radar image, which is formed in accordance with this algorithm, will be complex. Therefore, to display it, the modulus or square of the modulus is usually calculated [45] and it is this function that is taken for the assessment of the radar image, i.e.

$$\hat{I}_{MSAR}(\mathbf{r}) = \left| \int_0^T \int_0^T \dot{U}(t_1) W(t_1, t_2, \sigma(\mathbf{r})) \dot{S}_s^*(t_2, h, \mathbf{r}) dt_1 dt_2 \right|^2. \quad (6)$$

For the first time, the problem of synthesis of an algorithm for optimal recovery of the specific effective scattering surface and its solution with obtaining the MSAR algorithm were developed by V. K. Volosyuk [46].

Algorithm (6) corresponds to the following basic signal processing operations: forming the envelope of the reference signal $\dot{S}_s^*(t, \mathbf{r})$ for different range sections (the number of range sections is determined by a specific signal shape and antenna directivity patterns for transmission and reception); setting of the decorrelation filter, the impulse response of which is determined by the function $W(t_1, t_2, \sigma(\mathbf{r}))$ (in the optimal form, this function is adaptive, since it requires a priori knowledge of $\sigma(\mathbf{r})$); formation of observation envelopes $\dot{U}(t, \mathbf{r})$ for different parts of the range; performing double correlation processing operations in accordance with (6).

It should be noted that the most difficult operation in (6) is the formation of the function $W(t_1, t_2, \sigma(\mathbf{r}))$. However, in practice, it can be realized as the average value of $\sigma(\mathbf{r})$, which is typical for a certain type of underlying surface. In some cases, filtering can be neglected and go to a quasi-optimal signal processing algorithm. For this, it is necessary to introduce the following replacement in (6) $W(t_1, t_2, \mathbf{r}) = \delta(t_1 - t_2)$. In this case, the signal processing algorithm is reduced to the classical algorithm used in SAR [47, 48]

$$\hat{I}_{SAR}(\mathbf{r}) = \left| \int_0^T \dot{U}(t) \dot{S}_s^*(t, h, \mathbf{r}) dt \right|^2.$$

Note that algorithm (6) allows obtaining high spatial resolution for viewing angles $\pm(20^\circ \dots 50^\circ)$ from the direction to the nadir.

The block diagram that implements the MSAR algorithm will be given below as part of the complex for the formation of radar images.

B. Active ASR Imaging Algorithm

For the first time, the problem of synthesizing a signal processing algorithm in an active aperture synthesis system was formulated and partially solved in [15]. Its peculiarity lies in the fact that it is not the effective temperature of the underlying surface that is subject to recovery, as is typical for passive aperture synthesis systems, but the specific effective scattering surface, similar to active synthesis systems, for example, in MSAR. This makes it possible to form radar images of the same physical entity by different synthesis systems. Active systems of aperture synthesis are of particular importance when solving problems of forming radar images within $\pm 20^\circ$ of the nadir.

We will synthesize a signal processing algorithm in such a system. To achieve a high resolution in spatial coordinates, we will use a wideband signal, the model of which can be represented as a Gaussian process with zero mean as follows

$$s(t) = 2 \int_{F_{\min}}^{F_{\max}} \dot{N}(j2\pi f) \exp(j2\pi f t) df, \quad (7)$$

where F_{\max} and F_{\min} are the limits of operating frequencies;

$\dot{N}(j2\pi f)$ is the random spectral density of the complex amplitude;

t is the time;

f is the frequency.

As it is usually done in aperture synthesis systems, to receive the reflected signal, we will use an N -element antenna array with a non-equidistant spatially distributed arrangement of the phase centers of individual antennas. The position of the phase centers of the elements of the antenna array is determined by the Monte Carlo method.

According to fig. 1 let us determine the signal propagation delay time from the transmitter antenna to an elementary section of the underlying surface and then to the i -th ($i=1..N$) receiver antenna (the phase center is characterized by the end of the radius vector $\mathbf{r}'_i = (x'_i, y'_i)$, the beginning of which is at the phase center of the transmitter antenna)

$$t_{d,i}(\mathbf{r}, \mathbf{r}'_i) = (R(t, \cdot) + R_i(t, \cdot)) c^{-1}, \quad (8)$$

where $R(t, \cdot) = \sqrt{h^2 + (x_C - Vt)^2 + y_C^2}$,

$R_i(t, \cdot) = \sqrt{h^2 + (x_C - V_x t - x'_i - x'_{di})^2 + (y_C - y'_i - y'_{di})^2}$,
 (x'_i, y'_i) are the coordinates of the phase center of the i -th element of the antenna system, $i=1..Q$, (x'_{di}, y'_{di}) are the coordinates of the receiving aperture of the i -th element of the antenna system, which are counted from the end of the vector \mathbf{r}'_i .

Signal at the output of the i -th element of the receiving antenna system

$$\begin{aligned} s_i(t, \mathbf{r}') = & 2 \int_{-\infty}^{\infty} \int_{-\infty}^{\infty} \int_{F_{\min}}^{F_{\max}} I(\mathbf{r}'_{di}) \times \\ & \times \dot{F}_C(2\pi f, \mathbf{r}) \dot{G}(2\pi f, Vt, \mathbf{r}) \dot{N}(j2\pi f) \times \\ & \times \exp(j2\pi f(t - t_{d,i}(\mathbf{r}, \mathbf{r}'_i))) df d\mathbf{r}'_{di} dr, \end{aligned} \quad (9)$$

where $\dot{G}(2\pi f, Vt, \mathbf{r})$ is the complex radiation pattern of the transmitter, which is recalculated to the elements of the underlying surface;

$I(\mathbf{r}'_{di})$ is the amplitude-phase distribution in the aperture of the i -th element of the antenna system;

$\dot{F}_C(2\pi f, \mathbf{r})$ is the complex reflection coefficient of an elementary section of the underlying surface centered at the end of the vector \mathbf{r} .

We rearrange the observation equation at the output of each element of the antenna system by a vector:

$$\mathbf{u}(t) = \{s_i(t, \mathbf{r}') + n_i(t)\}_{i=1}^N, \quad (10)$$

where

$$n_i(t) = 2 \int_{F_{\min}}^{F_{\max}} \dot{N}_{n,i}(j2\pi f) \exp(j2\pi f t) df, \quad (11)$$

is the internal noise of the i -th receiving channel, $\dot{N}_{n,i}(j2\pi f)$ is the random spectral density of the complex amplitude of the noise in the i -th channel.

The physical nature of noise is such that it is a zero-mean Gaussian process. There is no cross-correlation of noise between different channels, because in different channels the noise is statistically independent.

Full information about the observation is contained in the matrix of correlation functions

$$\mathbf{R}(t_1, t_2, \sigma(\mathbf{r})) = \langle \mathbf{u}(t_1) \mathbf{u}^T(t_2) \rangle, \quad (12)$$

where "T" is the transposition operator;

$\sigma(\mathbf{r})$ is the radar cross section of the underlying surface.

Substituting (9) and (11) in (10), and (10) in (12) and rewrite the matrix of correlation functions in the following form

$$\begin{aligned} \mathbf{R}(t_1, t_2, \sigma) &= \langle \mathbf{u}^T(t_1) \mathbf{u}(t_2) \rangle = \\ &= \left\{ \begin{array}{l} \int_{-\infty}^{\infty} \int_{F_{\min}}^{F_{\max}} \sigma(f, \mathbf{r}) \exp(j2\pi f(t_1 - t_2)) \times \\ \times N(2\pi f) \dot{G}(2\pi f, Vt_1, \mathbf{r}) \dot{G}^*(2\pi f, Vt_2, \mathbf{r}) \times \\ \times \int_{-\infty}^{\infty} \int_{-\infty}^{\infty} I(\mathbf{r}'_{di}) I^*(\mathbf{r}'_{dl}) \times \\ \times \exp \left(-j2\pi f c^{-1} \left[R(t_1, \cdot) - R(t_2, \cdot) + \right. \right. \\ \left. \left. + R_i(t_1, \cdot) - R_i(t_2, \cdot) \right] \right) \times \\ \times d\mathbf{r}'_{di} d\mathbf{r}'_{dl} d\mathbf{r} df \end{array} \right\}_{i,l=1}^N + \\ &+ \mathbf{I}^N \int_{F_{\min}}^{F_{\max}} N_n(2\pi f) \exp(j2\pi f(t_1 - t_2)) df, \quad (13) \end{aligned}$$

where \mathbf{I}^N is the unit dimension matrix $N \times N$;

$N(2\pi f)$ and $N_n(2\pi f)$ are the spectral power densities of the signal and noise (we assume that the spectral power densities of the noise are the same in value in all channels, which is determined by the thermodynamic temperature of the input paths);

$\sigma(f, \mathbf{r})$ is the frequency-dependent specific effective scattering area of the underlying surface.

Function $\sigma(f, \mathbf{r})$ act as a radar image both at each of the individual frequencies, and in integral form at all frequencies.

Expression (13) is a mathematical model of the relationship between the statistical characteristics of the observation and the radar image.

We can find the signal processing algorithm by solving the likelihood equation

$$\begin{aligned} \frac{\delta}{\delta \sigma(\mathbf{r}')} \ln p(\mathbf{u}(t) | \sigma(f, \mathbf{r})) &= \frac{\delta}{\delta \sigma(\mathbf{r}')} \ln k(\sigma(f, \mathbf{r})) - \\ &- \frac{\delta}{\delta \sigma(\mathbf{r}')} \left\{ -\frac{1}{2} \int_0^T \int_0^T [\mathbf{u}(t_1) - \langle \mathbf{s}(t_1, \mathbf{r}') \rangle]^T \times \right. \\ &\times \mathbf{W}(t_1, t_2, \sigma(f, \mathbf{r})) [\mathbf{u}(t_2) - \langle \mathbf{s}(t_2, \mathbf{r}') \rangle] dt_1 dt_2 \left. \right\} = 0, \quad (14) \end{aligned}$$

where $k(\sigma(f, \mathbf{r}))$ is the function that depends on the radar image; $\langle \cdot \rangle$ are the statistical averaging brackets;

$\mathbf{W}(t_1, t_2, \sigma(f, \mathbf{r}))$ is a matrix that is inverse to the matrix of correlation functions, and which is found from the solution of an integral matrix equation

$\int_0^T \mathbf{R}(t, q) \mathbf{W}(q, \tau) dq = \mathbf{I}^N \delta(t - \tau)$, where $\delta(t - \tau)$ is a delta function.

From the solution of equation (14), we find the following signal processing algorithm in the active aperture synthesis system:

$$\begin{aligned} \hat{\mathbf{I}}_{AASR}(\mathbf{r}) &= \\ &= \sum_{i,l=1}^N \int_{F_{\min}}^{F_{\max}} \exp \left(-j \frac{\pi f}{hc} ((y_C - y'_i)^2 - (y_C - y'_l)^2) \right) \times \\ &\times N(2\pi f) V_{F-FR} \{u_p(t, \mathbf{r})\} V_{F-FR}^* \{u_l(t, \mathbf{r})\} df, \quad (15) \end{aligned}$$

where $V_{F-FR} \{\cdot\}$ is the Volosyuk-Fourier-Fresnel operator [45].

Algorithm (15) is quasi-optimal, since the operations of decorrelating observations are excluded from it to simplify the technical implementation of the radio complex.

Algorithm (15) implies the main operations of observation processing: the implementation of V_{F-FR} -transformations for observations in all channels (the observation record in the form $u_i(t, \mathbf{r})$ indicates that the signal in the i -th channel is "focused" on an elementary section of the underlying surface with the center at the end of the radius vector \mathbf{r} . Such "focusing" is provided in decorrelated filters, and after their elimination is implemented in wideband phase shifters); multiplication of complex conjugate processes focused on the same area of the surface, after V_{F-FR} -transformations in different channels; compensation of the interferometric factor, which naturally appears in the process of diagram formation in a rarefied antenna array (this operation is usually associated with aperture synthesis [49]); integration within the operating frequency band of the receiver and the addition of all output effects from different pairs of antennas.

It was shown in [50] that for the case when the channel of the probing signal is absent, solution (15) is reduced to the signal processing algorithm in the aperture synthesis system

$$\hat{\mathbf{T}}(\mathbf{r}) = \sum_{i,l=1}^N \int_{F_{\min}}^{F_{\max}} F \{u_i(t, \mathbf{r})\} F^{-1} \{u_l(t, \mathbf{r})\} df \quad (16)$$

where $F \{\cdot\}$ and $F^{-1} \{\cdot\}$ are the operators of the direct and inverse Fourier transform.

Similarly to (15) in (16), signal decorrelating filters are not applied. The initial effect of the radar that implements (16) will be a function proportional to the radio brightness temperature of the underlying surface.

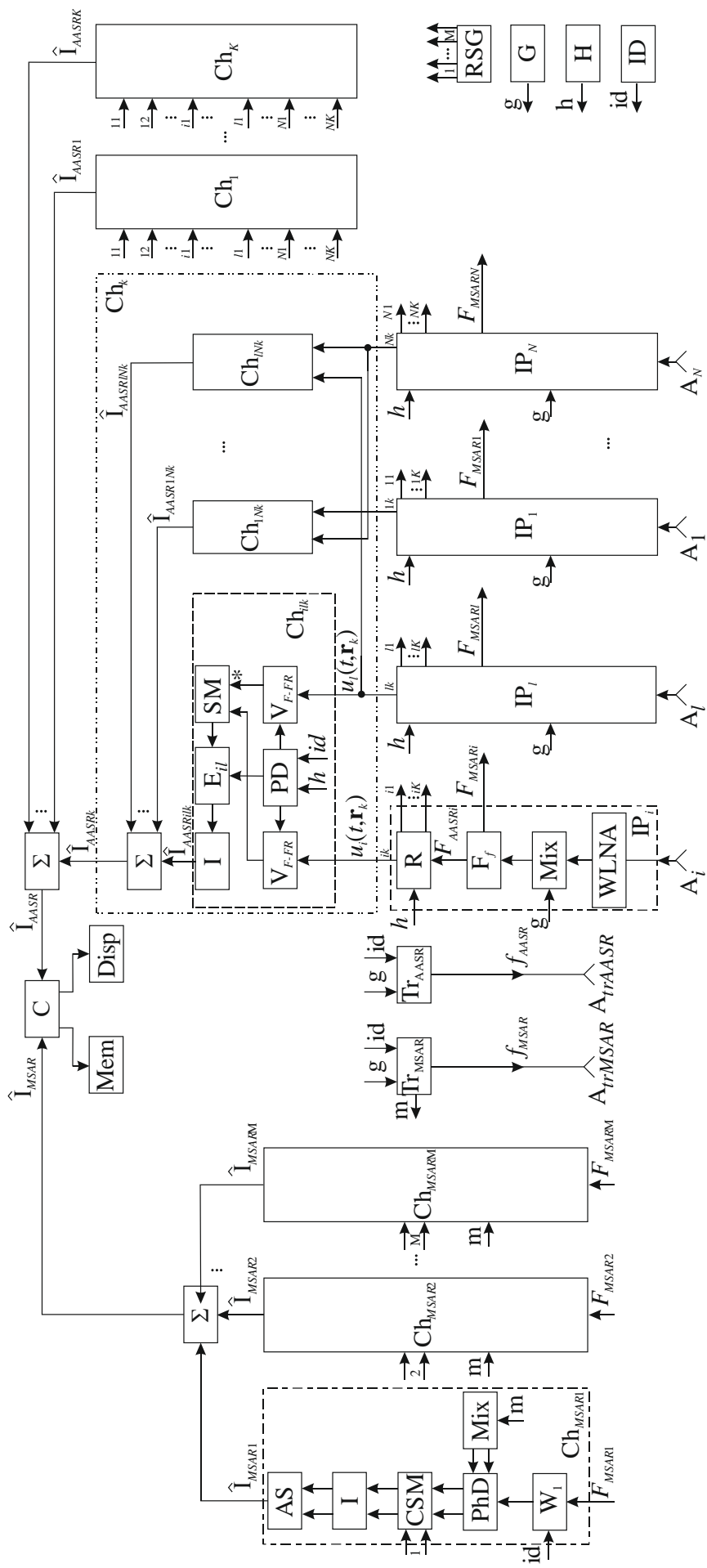


Fig. 2. Radiocomplex Block Diagram

Radiocomplex Block Diagram

According to the formulated task, we will design a structural diagram of the radio complex, which will provide the formation of a radar image within $\pm 50^\circ$ of the nadir. For this, it is necessary to implement signal processing algorithms (6) and (15).

In fig. 2 it is shown a block diagram of the complex for the formation of radar images.

In fig. 2, the following designations have been introduced: A_{trMSAR} is the modified SAR transmitter antenna; A_{trAASR} is the antenna of the AASR transmitter; A_i ($i=1..N$) are the receiving elements of the antenna system (all are involved in the operation of the AASR, and some, along the direction of movement of the aircraft, are involved in the work of the MSAR); ID is the block of initial data for the formation of the probing signal; Tr_{MSAR} and Tr_{AASR} are the transmitters of MSAR and AASR systems; IP_i is the receiver input path with frequency filtering; WLNA are the wideband low-noise amplifiers; Mix is the mixer with a filter for suppressing higher harmonics; F_f is the block for filtering (separating) signals by frequencies; f_{MSAR} and f_{AASR} are the operating frequencies of MSAR and AASR systems for radiated signals; designations F_{MSARI} and F_{AASRI} indicate that the signals of the MSAR and AASR systems in the i -th receive channel are transferred to intermediate frequencies; R is the block for dividing signals by range to sections of the underlying surface (uses a priori information about the flight altitude h from the H block); V_{F-FR} is the block of the Volosyuk-Fourier-Fresnel transformation; PD is the a priori data block; G is the heterodyne; RSG is the reference signal generator for MSAR; ID is the block of initial data; SM is the signal multiplication unit (one input is direct, and the other is complex conjugate, which is indicated by the corresponding sign *); E_{il} is the block of multiplication by a complex exponent, the argument of which is proportional to the distance between the i -th and l -th antennas; I is the integrator; Σ is the adder; W_m is the signal decorrelation unit; PhD is the phase detector; CSM is the complex signal multiplier; AS is the block for calculating the square of the module; \hat{I}_{AASR} is the assessment of the radar image at the AASR output; \hat{I}_{AASRik} is the evaluation of the radar image at the output of the signal processing channel from the i -th and l -th antennas for the k -th ($k=1..K$) range in the AASR; \hat{I}_{AASRk} is the estimation of the radar image for

the k -th range in the AASR; \hat{I}_{MSAR} is the evaluation of the radar image at the MSAR output; \hat{I}_{MSARM} is the estimation of the radar image for the m -th ($m=1..M$) range in MSAR; Ch_{ilk} is the formation channel for \hat{I}_{AASRik} ; Ch_k is the formation channel for \hat{I}_{AASRk} ; Ch_{MSARM} is the formation channel for \hat{I}_{MSARM} ; C is the computer; Mem is the memory for storing images; Disp is the display for displaying the image.

The complex works as follows. The transmitters Tr_{MSAR} and Tr_{AASR} generate and radiate signals through the antennas A_{trMSAR} and A_{trAASR} towards the underlying surface. The signals reflected by the surface are fed to the elements A_i of the receiving antenna system. All N elements of the receiving antenna system are involved in the operation of the AASR, and some of these elements (located along the direction of movement of the aircraft) are involved in the operation of the MSAR. Next, let's look at how AASR works. The signals from the outputs of the antennas go to the blocks IP_i , where they are amplified in WLNA, transferred to the intermediate frequency in the mixers Mix, which include filters for suppressing the higher components in the signal spectrum, then the signals go to the signal separation unit by frequency F_f and then to the range separation units R. Observation from the given range sections is fed to the Ch_{ilk} blocks, where the Volosyuk-Fourier-Fresnel V_{F-FR} transformation, multiplication of complex conjugate processes and compensation of the observation phase difference in E_{il} , which occurs due to the different paths of the reflected signals to the i -th and j -th antennas, are performed. After integration, one sample of the image \hat{I}_{AASRik} is formed.

Combining the outputs of the blocks Ch_{ilk} for all possible pairs il antennas provides the formation radar image at the output of the block Ch_k of the \hat{I}_{AASRk} for k -th ($k=1..K$) section of the range. After combining in the adder all the range elements into a line of the image of the observation area within $\pm 20^\circ$ from the nadir, it is fed to computer C and then stored in Mem and can be displayed on the Disp display.

Some AASR blocks (antennas, mixers, frequency separators) are common to MSAR as well. Further, the signals at frequencies F_{MSARI} and filtered by range are fed to the Ch_{MSARM} blocks for forming images in the zone $\pm(20^\circ..50^\circ)$ from the nadir. In these blocks, whitening of signals in filters W_m , phase detection in PhD blocks and correlation processing in CSM and I,

as well as the formation of a square of the image module in AS are performed. At the outputs of Ch_{MSARm} element of the radar image $\hat{\mathbf{I}}_{\text{MSARm}}$ is formed for the m -th section of the range. It should be noted that the number of ranges for MSAR and AASR may differ. Images of different ranges of range are combined into a line for evaluating the radar image $\hat{\mathbf{I}}_{\text{MSAR}}$ and fed to a computer.

It should be noted that the issues of the accuracy of image formation are often investigated in the problems of synthesizing radio complexes. These questions are beyond the scope of this article, but they can be solved both by using optimization methods, when the so-called potential values of accuracy are obtained [45], and directly from navigation [51-53] or other data [54-56], by indirect methods of image processing.

Conclusions

In this work, the structure of a radar complex for forming an image of the underlying surface in a swath of $\pm 50^\circ$ from the direction to the nadir is synthesized for the first time. The peculiarity of the complex is as follows:

- the presence of two modes of operation - MSAR and AASR, which respectively provide survey in the range of angles $\pm(50^\circ \dots 20^\circ)$ and $\pm 20^\circ$ from the nadir, and their combined use gives a continuous image in the swath of $\pm 50^\circ$ from the nadir;

- the use of ultra-wideband probing signals and, accordingly, the same channels of the signal processing receiver, allows obtaining high image resolution in spatial coordinates.

It is assumed that this complex can be used from aircraft or space carriers.

Acknowledgement. The work was supported by the Ministry of Education and Science of Ukraine, the state registration numbers of the projects are 0119U100968, 0120U102082 and 0121U109598.

References (GOST 7.1:2006)

1. *Three-state locally adaptive texture preserving filter for radar and optical image processing* [Text] / O. V. Tsymbal, V. V. Lukin, N. N. Ponomarenko, A. A. Zelensky, K. O. Egiazarian, J. T. Astola // *Eurasip Journal on Applied Signal Processing*. – 2005. – No. 8. – P. 1185-1204. DOI: 10.1155/ASP.2005.1185.
2. *Image informative maps for estimating noise standard deviation and texture parameters* [Text] / B. Vozel, M. Uss, V. Lukin, S. Abramov, I. Baryshev, K. Chehdi // *Eurasip Journal on Advances in Signal Processing*, 2011. DOI: 10.1155/2011/806516.

3. *Super-resolution SAR imaging: Optimal algorithm synthesis and simulation results* [Text] / V. F. Kravchenko, B. G. Kutuza, V. K. Volosyuk, V. V. Pavlikov, S. S. Zhyla // *Progress In Electromagnetics Research Symposium – Spring. PIERS*. – 2017. – P. 419-425. DOI: 10.1109/PIERS.2017.8261776.

4. *Pavlikov, V. V. Algorithm for radiometric imaging by ultrawideband systems of aperture synthesis* [Text] / V. V. Pavlikov, Nguen Van Kiem, O. M. Tymoshchuk // *IEEE Radar Methods and Systems Workshop. RMSW*. – 2016. – P. 103-106. DOI: 10.1109/RMSW.2016.7778561.

5. *Multiantenna radiometric complex for high resolution imaging: Synthesis of algorithm for optimal UWB signal processing and development of functional flow block diagram* [Text] / V. F. Kravchenko, B. G. Kutuza, V. K. Volosyuk, V. V. Pavlikov, Nguen Van Kiem // *Progress In Electromagnetics Research Symposium – Spring. PIERS*. – 2017. – P. 426-430. DOI: 10.1109/PIERS.2017.8261777.

6. *Pavlikov, V. V. Spectral method for the spatio-spectral sensitivity domain filling in aperture synthesis system* [Text] / V. V. Pavlikov, Nguen Van Kiem, O. M. Tymoshchuk, // *8th International Conference on Ultrawideband and Ultrashort Impulse Signals. UWBUSIS*. – 2016. – P. 124-127. DOI: 10.1109/UWBUSIS.2016.7724167.

7. Еремеєв, О. І. Комбінована метрика візуальної якості зображень дистанційного зондування на основі нейронної мережі [Текст] / О. І. Еремеєв, В. В. Лукін, К. Окарма // *Радіоелектронні і комп’ютерні системи*. – 2020. – № 4(96). – С. 4-15. DOI: 10.32620/reks.2020.4.01

8. *Adaptive DCT-based filtering of images corrupted by spatially correlated noise* [Text] / N. N. Ponomarenko, V. V. Lukin, A. A. Zelensky, J. T. Astola, K. O. Egiazarian // *Proceedings of SPIE – the International Society for Optical Engineering* 6812, 68120W (2008). DOI: 10.1117/12.764893.

9. *Prediction of filtering efficiency for DCT-based image denoising* [Text] / S. Abramov, S. Krivenko, A. Roenko, V. Lukin, I. Djurović, M. Chobanu // *2nd Mediterranean Conference on Embedded Computing. MECO*. – 2013. – P. 97-100. DOI: 10.1109/MECO.2013.6601327.

10. *Gorovyj, I. M. Efficient data focusing and trajectory reconstruction in airborne SAR systems* [Text] / I. M. Gorovyj, O. O. Bezvesilniy, D. M. Vavriv // *Signal Processing Symposium. SPSympo*. – 2015. – P. 1-5. DOI: 10.1109/SPS.2015.7168271.

11. *Villano, M. Advanced spaceborne SAR systems with planar antenna* [Text] / M. Villano, G. Krieger,

- A. Moreira // IEEE Radar Conference. RadarConf. – 2017. – P. 152-156. DOI: 10.1109/RADAR.2017.7944188.
12. Desruelles, G. Submillimetric high resolution passive imaging system using synthesis aperture technique [Text] / G. Desruelles, N. Rolland, P. Rolland // 7th European Radar Conference. – 2010. – P. 280-283.
13. On the use of passive microwave remote sensing by airborne platforms [Text] / M. Peichl, S. Dill, M. Jirousek, E. Schreiber // 16th International Radar Symposium. IRS. – 2015. – P. 225-230. DOI: 10.1109/IRS.2015.7226382.
14. Методика определения поля обнаружения беспилотных летательных аппаратов наземным наблюдателем [Текст] / С. К. Абрамов, В. В. Абрамова, К. Д. Абрамов, В. В. Лукин, В. В. Бондарь, И. В. Калужинов // Радиоелектронні і комп'ютерні системи. – 2020. – № 3(95). – С. 36-42. DOI: 10.32620/reks.2020.3.04.
15. A new method of multi-frequency active aperture synthesis for imaging of SAR blind zone under aerospace vehicle [Text] / V. Pavlikov, V. Volosyuk, S. Zhyla, Nguen Van Huu, Nguen Van Kiem // 14th International Conference The Experience of Designing and Application of CAD Systems in Microelectronics. CADSM. – 2017. – P. 118-120. DOI: 10.1109/CADSM.2017.7916099.
16. Active Aperture Synthesis Radar for High Spatial Resolution Imaging [Text] / V. V. Pavlikov, V. K. Volosyuk, S. S. Zhyla, Nguen Van Huu // 9th International Conference on Ultrawideband and Ultrashort Impulse Signals. UWBUSIS. – 2018. – P. 252-255. DOI: 10.1109/UWBUSIS.2018.8520021.
17. Signal Processing Algorithm for Active Aperture Synthesis Systems [Text] / V. Pavlikov, V. Volosyuk, S. Zhyla, Nguen Van Huu, Nguen Van Kiem, A. Sobkolov // IEEE 15th International Conference on the Experience of Designing and Application of CAD Systems. CADSM. – 2019. – P. 1-4. DOI: 10.1109/CADSM.2019.8779350.
18. Imaging by aerospace radar systems with active aperture synthesis [Text] / O. A. Daki, Nguen Van Huu, V. V. Pavlikov, A. D. Sobkolov, O. M. Tymoshchuk // Telecommunications and Radio Engineering. – 2019. – Vol. 78, no. 14. – P. 1233-1247. DOI: 10.1615/TelecomRadEng.v78.i14.20.
19. Algorithm of Formation Radio Images from Aerospace Carriers [Text] / V. Pavlikov, V. Volosyuk, M. Nechyporuk, A. Sobkolov, O. Odokienko, E. Tserne // IEEE Ukrainian Microwave Week. UkrMW. – 2020. – P. 54-58. DOI: 10.1109/UkrMW49653.2020.9252702.
20. Pavlikov, V. V. Ultra-wideband Passive radars Fundamental Theory and Applications [Text] / V. V. Pavlikov, V. K. Volosyuk, S. S. Zhyla // IEEE 17th International Conference on Mathematical Methods in Electromagnetic Theory. MMET. – 2018. – P. 1-6. DOI: 10.1109/MMET.2018.8460251.
21. Quasioptimal Spatiotemporal Signal Processing Algorithm for Radar Imaging [Text] / V. V. Pavlikov, M. V. Nechyporuk, Nguen Van Huu, A. D. Sobkolov // IEEE 15th International Conference on Advanced Trends in Radioelectronics, Telecommunications and Computer Engineering. TCSET. – 2020. – P. 559-564. DOI: 10.1109/TCSET49122.2020.235495.
22. Holliday, R. A lightweight, ultra wideband polarimetric W-band radar with high resolution for environmental applications [Text] / R. Holliday, M. Rhys-Roberts, D. A. Wynn // European Radar Conference. – 2006. – P. 194-197. DOI: 10.1109/EURAD.2006.280307.
23. Fu, J. A fiber-distributed multistatic ultra-wideband radar [Text] / J. Fu, X. Chen, S. Pan // 14th International Conference on Optical Communications and Networks. ICOON. – 2015. – P. 1-3. DOI: 10.1109/ICOON.2015.7203608.
24. Chirov, D. S. Assessment of the Accuracy of Determining the Coordinates and Speed of Small-Size UAV of a Multi-Position Radar with Omnidirectional Antenna Elements [Text] / D. S. Chirov, Y. A. Kochetkov // Systems of Signals Generating and Processing in the Field of on Board Communications. – 2020. – P. 1-6. DOI: 10.1109/IEEECONF48371.2020.9078571.
25. Yang, Y. See-through-wall imaging using ultra wideband short-pulse radar system [Text] / Y. Yang, A. E. Fathy // IEEE Antennas and Propagation Society International Symposium. – 2005. – Vol. 3B. – P. 334-337. DOI: 10.1109/APS.2005.1552508.
26. FMCW ultra-wideband radar for through-the-wall detection of human beings [Text] / N. Maaref, P. Millot, C. Pichot, O. Picon // International Radar Conference "Surveillance for a Safer World". RADAR. – 2009. – P. 1-5.
27. Portable Low-Power Fully Digital Radio-Frequency Direct-Transceiving See-Through-Wall Radar [Text] / P. Li, F. Zhou, P. Luo, M. Liu // IEEE Access. – 2020. – Vol. 8. – P. 163298-163307. DOI: 10.1109/ACCESS.2020.3019966.
28. Davis, M. E. Challenges of ultra wideband, multi-mode radar [Text] / M. E. Davis // Proceedings of IEEE CIE International Conference on Radar. – 2011. – P. 5-8. DOI: 10.1109/CIE-Radar.2011.6159706.

29. Chen, K. M. Ultra-wideband/short-pulse radar for target identification and detection-laboratory study [Text] / K. M. Chen // Proceedings International Radar Conference. – 1995. – P. 450-455. DOI: 10.1109/RADAR.1995.522590.
30. Kharchenko, V. Concepts of green IT engineering: Taxonomy, Principles and implementation [Text] / V. Kharchenko, O. Illiashenko // Studies in Systems, Decision and Control. – 2016. – Vol. 74. – P. 3-19. DOI: 10.1007/978-3-319-44162-7_1.
31. The new method of antenna aperture synthesis with received signal decorrelation [Text] / V. V. Volosyuk, V. F. Kravchenko, B. G. Kutuza, V. V. Pavlikov // 10th European Conference on Synthetic Aperture Radar. EUSAR. – 2014. – P. 1-4. EID: 2-s2.0-84994234354.
32. Fundamental Principles of Radar [Text] / H. Rahman. – 1st ed. – Boca Raton : CRC Press, 2019. – 339 p.
33. Huimin, L. Analysis of a combined waveform of linear frequency modulation and phase coded modulation [Text] / L. Huimin, Z. Jingya // 11th International Symposium on Antennas, Propagation and EM Theory. ISAPE. – 2016. – P. 539-541. DOI: 10.1109/ISAPE.2016.7834008.
34. Linear frequency modulation waveform synthesis [Text] / K. Patel, U. Neelakantan, S. Gangele, J. G. Vacchani, N. M. Desai // IEEE Students' Conference on Electrical, Electronics and Computer Science. – 2012. – P. 1-4. DOI: 10.1109/SCEECS.2012.6184744.
35. Roy, T. M. D. Efficient Digital Implementation of Non Linear Frequency Modulation for Radar Applications [Text] / T. M. D. Roy, L. G. M. Prakasam // IEEE MTT-S International Microwave and RF Conference. IMaRC. – 2018. – P. 1-4. DOI: 10.1109/IMaRC.2018.8877350.
36. Peng, Y. JLHS: A Joint Linear Frequency Modulation and Hyperbolic Frequency Modulation Approach for Speed Measurement [Text] / Y. Peng // IEEE Access. – 2020. – Vol. 8. – P. 205316-205326. DOI: 10.1109/ACCESS.2020.3037801.
37. Ultrawideband Radar: Applications and Design [Text] / J. D. Taylor. – Boca Raton : CRC Press, 2012. – 536 p.
38. Sabath, F. Definition and classification of ultra-wideband signals and devices [Text] / F. Sabath, E. L. Mokole, S. N. Samaddar // URSI Radio Science Bulletin. – 2005. – Vol. 2005, no. 313. – P. 12-26. DOI: 10.23919/URSIRSB.2005.7909522.
39. Mughal, M. O. Signal Classification and Jamming Detection in Wide-Band Radios Using Naïve Bayes Classifier [Text] / M. O. Mughal, S. Kim // IEEE Communications Letters. – 2018. – Vol. 22, no. 7. – P. 1398-1401. DOI: 10.1109/LCOMM.2018.2830769.
40. Friedlander, B. Direction finding for wideband signals using an interpolated array [Text] / B. Friedlander, A. J. Weiss // Conference Record of the Twenty-Fifth Asilomar Conference on Signals, Systems & Computers. – 1991. – Vol. 1. – P. 583-587 DOI: 10.1109/ACSSC.1991.186515.
41. Noureddine, L. A joint space-time estimation algorithm for wideband signals with high resolution capabilities [Text] / L. Noureddine, H. Ferid, G. Ali // 6th International Multi-Conference on Systems, Signals and Devices. – 2009. – P. 1-5. DOI: 10.1109/SSD.2009.4956659.
42. Hippenstiel, R. Classification of wideband transient signals using spectral-based techniques [Text] / R. Hippenstiel, M. P. Fargues // Proceedings of 27th Asilomar Conference on Signals, Systems and Computers. – 1993. – Vol. 2. – P. 1479-1483. DOI: 10.1109/ACSSC.1993.342367.
43. Chernogor, L. F. The modeling of ultra-wideband signals and processes [Text] / L. F. Chernogor, O. V. Lazorenko // 6th International Conference on Ultrawideband and Ultrashort Impulse Signals. – 2012. – P. 246-248. DOI: 10.1109/UWBUSIS.2012.6379795.
44. Chernogor, L. F. New models of the fractal ultra-wideband signals [Text] / L. F. Chernogor, O. V. Lazorenko, A. A. Onishchenko // 8th International Conference on Ultrawideband and Ultrashort Impulse Signals. UWBUSIS. – 2016. – P. 89-92. DOI: 10.1109/UWBUSIS.2016.7724158.
45. Волосюк, Б. К. Статистическая теория радиотехнических систем дистанционного зондирования и радиолокации [Текст] / Б. К. Волосюк, В. Ф. Кравченко. – М. : Физматлит, 2008. – 704 с.
46. Volosyuk, V. K. Optimal estimation of the radar cross-section for the stochastic surface models [Text] / V. K. Volosyuk, A. V. Ksendzuk, S. N. Eskov // Fourth International Kharkov Symposium 'Physics and Engineering of Millimeter and Sub-Millimeter Waves'. Symposium Proceedings (Cat. No.01EX429). – 2001. – Vol. 1. – P. 438-440.
47. Near-Field MIMO-SAR Millimeter-Wave Imaging With Sparsely Sampled Aperture Data [Text] / M. E. Yanik, M. Torlak // IEEE Access. – 2019. – Vol. 7. – P. 31801-31819, DOI: 10.1109/ACCESS.2019.2902859.
48. Spotlight SAR Imaging with Sufficient Cyclic Prefix-OFDM Waveform [Text] / G. Sharma, A. B. Raj // 2020 International Conference on Smart Electronics

and Communication. ICOSEC. – 2020. – P. 625-630. DOI: 10.1109/ICOSEC49089.2020.9215293.

49. Active-Passive Radar for Radar Imaging from Aerospace Carriers [Text] / V. Pavlikov, V. Volosyuk, S. Zhyla, E. Tserne, O. Shmatko, A. Sobkolov // IEEE 19th International Conference on Smart Technologies. EUROCON. – 2021. – P. 18-24. DOI: 10.1109/EUROCON52738.2021.9535619.

50. Development of Broadband Criterion for Spatially Distributed Radio Systems Synthesis [Text] / V. Pavlikov, V. Volosyuk, S. Zhyla, A. Sobkolov, O. Odokienko, E. Tserne, O. Shmatko, A. Sobkolov // IEEE 3rd Ukrainian Conference on Electrical and Computer Engineering. UKRCON. – 2021. – P. 232-236.

51. Kuzmenko, N. S. An Accuracy and Availability Estimation of Aircraft Positioning by Navigational Aids [Text] / N. S. Kuzmenko, I. V. Ostroumov, K. Marais // In Proceedings of the 2018 IEEE 5th International Conference on Methods and Systems of Navigation and Motion Control. MSNMC. – 2018. – P. 36–40. DOI: 10.1109/MSNMC.2018.8576276.

52. DME/DME position and velocity estimation [Text] / K. Sezginer, M. Güll, A. Beköz, Y. B. Özer, C. Kasnakoglu // 26th Signal Processing and Communications Applications Conference (SIU). – 2018. – P. 1-4. DOI: 10.1109/SIU.2018.8404414.

53. Ostroumov, I. V. Compatibility analysis of multi signal processing in APNT with current navigation infrastructure [Text] / I. V. Ostroumov, N. S. Kuzmenko // Telecommunications and Radio Engineering. – 2018. – Vol. 77, no. 3. – P. 211-223. DOI: 10.1615/TelecomRadEng.v77.i3.30.

54. Heteroskedasticity Analysis During Operational Data Processing of Radio Electronic Systems [Text] / M. Zaliskiy, O. Solomentsev, O. Shcherbyna, I. Ostroumov, O. Sushchenko, Y. Averyanova // Data Science and Security. Lecture Notes in Networks and Systems / S. Shukla, A. Unal, Kureethara J. Varghese, D. K. Mishra, D. S. Han (Eds.). – Singapore: Springer, 2021. – Vol. 290. – P. 168-175. DOI: 10.1007/978-981-16-4486-3_18.

55. Three-State Locally Adaptive Texture Preserving Filter for Radar and Optical Image Processing [Text] / O. V. Tsymbal, V. V. Lukin, N. N. Ponomarenko et al. // EURASIP J. Adv. Signal Process. 851609. – 2005. DOI: 10.1155/ASP.2005.1185.

56. Image Informative Maps for Estimating Noise Standard Deviation and Texture Parameters [Text] / M. Uss, B. Vozel, V. Lukin et al. // EURASIP J. Adv. Signal Process. 806516. – 2011. DOI: 10.1155/2011/806516.

References (BSI)

1. Tsymbal, O. V., Lukin, V. V., Ponomarenko, N. N., Zelensky, A. A., Egiazarian, K. O., Astola, J. T. Three-state locally adaptive texture preserving filter for radar and optical image processing. *Eurasip Journal on Applied Signal Processing*, 2005, no. 8, pp. 1185-1204. DOI: 10.1155/ASP.2005.1185.
2. Vozel, B., Uss, M., Lukin, V., Abramov, S., Baryshev, I., Chehdi, K. Image informative maps for estimating noise standard deviation and texture parameters. *Eurasip Journal on Advances in Signal Processing*, 2011, DOI: 10.1155/2011/806516.
3. Kravchenko, V. F., Kutuza, B. G., Volosyuk, V. K., Pavlikov, V. V., Zhyla, S. S. Super-resolution SAR imaging: Optimal algorithm synthesis and simulation results. *Progress In Electromagnetics Research Symposium – Spring (PIERS)*, 2017, pp. 419-425. DOI: 10.1109/PIERS.2017.8261776.
4. Pavlikov, V. V., Nguen Van Kiem, Tymoshchuk, O. M. Algorithm for radiometric imaging by ultrawideband systems of aperture synthesis. *IEEE Radar Methods and Systems Workshop (RMSW)*, 2016, pp. 103-106. DOI: 10.1109/RMSW.2016.7778561.
5. Kravchenko, V. F., Kutuza, B. G., Volosyuk, V. K., Pavlikov, V. V., Van, K. N. Multiantenna radiometric complex for high resolution imaging: Synthesis of algorithm for optimal UWB signal processing and development of functional flow block diagram. *Progress In Electromagnetics Research Symposium – Spring (PIERS)*, 2017, pp. 426-430. DOI: 10.1109/PIERS.2017.8261777.
6. Pavlikov, V. V., Nguen Van Kiem, Tymoshchuk, O. M. Spectral method for the spatio-spectral sensitivity domain filling in aperture synthesis system. *8th International Conference on Ultrawideband and Ultrashort Impulse Signals (UWBUSIS)*, 2016, pp. 124-127. DOI: 10.1109/UWBUSIS.2016.7724167.
7. Ieremeiev, O., Lukin, V., Okarma, K. Kombinovana metryka vizual'noyi yakosti zobrazen' dystantsiynoho zonduvannya na osnovi nevronnoyi merezhi [Combined visual quality metric of remote sensing images based on neural network]. *Radioelektronni i komp'uterni sistemi – Radioelectronic and computer systems*, 2020, no. 4(96), pp. 4-15. DOI: 10.32620/reks.2020.4.01.
8. Ponomarenko, N. N., Lukin, V. V., Zelensky, A. A., Astola, J. T., Egiazarian, K. O. Adaptive DCT-based filtering of images corrupted by spatially correlated noise. *Proceedings of SPIE - the International Society for Optical Engineering*, 2008, 6812, 68120W. DOI: 10.1117/12.764893.

9. Abramov, S., Krivenko, S., Roenko, A., Lukin, V., Djurović, I., Chobanu, M. Prediction of filtering efficiency for DCT-based image denoising. *2nd Mediterranean Conference on Embedded Computing (MECO)*, 2013, pp. 97-100. DOI: 10.1109/MECO.2013.6601327.
10. Gorovyi, I. M., Bezvesilnyi, O. O., Vavriv, D. M. Efficient data focusing and trajectory reconstruction in airborne SAR systems. *Signal Processing Symposium (SPSympo)*, 2015, pp. 1-5. DOI: 10.1109/SPS.2015.7168271
11. Villano, M., Krieger, G., Moreira, A. Advanced spaceborne SAR systems with planar antenna. *IEEE Radar Conference (RadarConf)*, 2017, pp. 152-156. DOI: 10.1109/RADAR.2017.7944188.
12. Desruelles, G., Rolland, N., Rolland, P. Submillimetric high resolution passive imaging system using synthesis aperture technique. *7th European Radar Conference*, 2010, pp. 280-283.
13. Peichl, M., Dill, S., Jirousek, M., Schreiber, E. On the use of passive microwave remote sensing by airborne platforms. *16th International Radar Symposium (IRS)*, 2015, pp. 225-230. DOI: 10.1109/IRS.2015.7226382.
14. Abramov, S. K., Abramova, V. V., Abramov, K. D., Lukin, V. V., Bondar, V. V., Kaluzhinov, I. V. Metodika opredelenija polja obnaruzhenija bespilotnyh letatel'nyh apparatov nazemnym nabljudatelem [Technique of detection field estimating for unmanned aerial vehicles by a ground observer]. *Radioelektronni i kom'uterni sistemi – Radioelectronic and computer systems*, 2020, no. 3(95), pp. 36-42. DOI: 10.32620/reks.2020.3.04.
15. Pavlikov, V., Volosyuk, V., Zhyla, S., Nguen Van Huu, Nguen Van Kiem A new method of multi-frequency active aperture synthesis for imaging of SAR blind zone under aerospace vehicle. *14th International Conference The Experience of Designing and Application of CAD Systems in Microelectronics (CADSM)*, 2017, pp. 118-120. DOI: 10.1109/CADSM.2017.7916099.
16. Pavlikov, V. V., Volosyuk, V. K., Zhyla, S. S., Van, Huu Nguen Active Aperture Synthesis Radar for High Spatial Resolution Imaging. *9th International Conference on Ultrawideband and Ultrashort Impulse Signals (UWBUSIS)*, 2018, pp. 252-255. DOI: 10.1109/UWBUSIS.2018.8520021.
17. Pavlikov, V., Volosyuk, V., Zhyla, S., Nguen Van Huu, Nguen Van Kiem, Sobkolov, A. Signal Processing Algorithm for Active Aperture Synthesis Systems. *IEEE 15th International Conference on the Experience of Designing and Application of CAD Systems (CADSM)*, 2019, pp. 1-4. DOI: 10.1109/CADSM.2019.8779350.
18. Daki, O. A., Nguen Van Huu, Pavlikov, V. V., Sobkolov, A. D., Tymoshchuk, O. M. Imaging by aerospace radar systems with active aperture synthesis. *Telecommunications and Radio Engineering*, 2019, vol. 78, no. 14, pp. 1233-1247. DOI: 10.1615/TelecomRadEng.v78.i14.20.
19. Pavlikov, V., Volosyuk, V., Nechyporuk, M., Sobkolov, A., Odokienko, O., Tserne, E. Algorithm of Formation Radio Images from Aerospace Carriers. *IEEE Ukrainian Microwave Week (UkrMW)*, 2020, pp. 54-58. DOI: 10.1109/UkrMW49653.2020.9252702.
20. Pavlikov, V. V., Volosyuk, V. K., Zhyla, S. S. Ultra-wideband Passive radars Fundamental Theory and Applications. *IEEE 17th International Conference on Mathematical Methods in Electromagnetic Theory (MMET)*, 2018, pp. 1-6. DOI: 10.1109/MMET.2018.8460251.
21. Pavlikov, V. V., Nechyporuk, M. V., Nguen Van Huu, Sobkolov, A. D. Quasioptimal Spatiotemporal Signal Processing Algorithm for Radar Imaging. *IEEE 15th International Conference on Advanced Trends in Radioelectronics, Telecommunications and Computer Engineering (TCSET)*, 2020, pp. 559-564. DOI: 10.1109/TCSET49122.2020.235495.
22. Holliday, R., Rhys-Roberts, M., Wynn, D. A. A lightweight, ultra wideband polarimetric W-band radar with high resolution for environmental applications. *European Radar Conference*, 2006, pp. 194-197. DOI: 10.1109/EURAD.2006.280307.
23. Fu, J., Chen, X., Pan, S. A fiber-distributed multistatic ultra-wideband radar. *14th International Conference on Optical Communications and Networks (ICOON)*, 2015, pp. 1-3. DOI: 10.1109/ICOON.2015.7203608.
24. Chirov, D. S., Kochetkov, Y. A. Assessment of the Accuracy of Determining the Coordinates and Speed of Small-Size UAV of a Multi-Position Radar with Omnidirectional Antenna Elements. *Systems of Signals Generating and Processing in the Field of on Board Communications*, 2020, pp. 1-6. DOI: 10.1109/IEEECONF48371.2020.9078571.
25. Yang, Y., Fathy, A. E. See-through-wall imaging using ultra wideband short-pulse radar system. *IEEE Antennas and Propagation Society International Symposium*, 2005, vol. 3B, pp. 334-337. DOI: 10.1109/APS.2005.1552508.
26. Maaref, N., Millot, P., Pichot C., Picon, O. FMCW ultra-wideband radar for through-the-wall detection of human beings. *International Radar Conference "Surveillance for a Safer World" (RADAR 2009)*, 2009, pp. 1-5.

27. Li, P., Zhou, F., Luo, P. Liu, M. Portable Low-Power Fully Digital Radio-Frequency Direct-Transceiving See-Through-Wall Radar. *IEEE Access*, 2020, vol. 8, pp. 163298-163307, DOI: 10.1109/ACCESS.2020.3019966.
28. Davis, M. E. Challenges of ultra wideband, multi-mode radar. Proceedings of IEEE CIE International Conference on Radar, 2011, pp. 5-8. DOI: 10.1109/CIE-Radar.2011.6159706.
29. Chen, K. M. Ultra-wideband/short-pulse radar for target identification and detection-laboratory study. *Proceedings International Radar Conference*, 1995, pp. 450-455. DOI: 10.1109/RADAR.1995.522590.
30. Kharchenko, V., Illiashenko, O. Concepts of green IT engineering: Taxonomy, Principles and implementation. *Studies in Systems, Decision and Control*, 2016, vol. 74, pp. 3-19. DOI: 10.1007/978-3-319-44162-7_1.
31. Volosyuk, V. V., Kravchenko, V. F., Kutuza, B. G., Pavlikov, V. V. The new method of antenna aperture synthesis with received signal decorrelation. *10th European Conference on Synthetic Aperture Radar (EUSAR 2014)*, 2014, pp. 1-4. EID: 2-s2.0-84994234354.
32. Rahman, H. *Fundamental Principles of Radar*. Boca Raton, CRC Press Publ., 2019. 339 p.
33. Huimin, L., Jingya, Z. Analysis of a combined waveform of linear frequency modulation and phase coded modulation. *11th International Symposium on Antennas, Propagation and EM Theory (ISAPE)*, 2016, pp. 539-541. DOI: 10.1109/ISAPE.2016.7834008.
34. Patel, K., Neelakantan, U., Gangele, S., Vacchani, J. G., Desai, N. M. Linear frequency modulation waveform synthesis. *IEEE Students' Conference on Electrical, Electronics and Computer Science*, 2012, pp. 1-4. DOI: 10.1109/SCECS.2012.6184744.
35. Roy, T. M. D., Prakasam, L. G. M. Efficient Digital Implementation of Non Linear Frequency Modulation for Radar Applications. *IEEE MTT-S International Microwave and RF Conference (IMaRC)*, 2018, pp. 1-4. DOI: 10.1109/IMaRC.2018.8877350.
36. Peng, Y. JLHS: A Joint Linear Frequency Modulation and Hyperbolic Frequency Modulation Approach for Speed Measurement. *IEEE Access*, 2020, vol. 8, pp. 205316-205326. DOI: 10.1109/ACCESS.2020.3037801.
37. Taylor, J. D. *Ultrawideband Radar: Applications and Design*. Boca Raton, CRC Press Publ., 2012. 536 p.
38. Sabath, F., Mokole, E. L., Samaddar, S. N. Definition and classification of ultra-wideband signals and devices. *URSI Radio Science Bulletin*, 2005, vol. 2005, no. 313, pp. 12-26. DOI: 10.23919/URSIRSB.2005.7909522.
39. Mughal, M. O., Kim, S. Signal Classification and Jamming Detection in Wide-Band Radios Using Naïve Bayes Classifier. *IEEE Communications Letters*, 2018, vol. 22, no. 7, pp. 1398-1401. DOI: 10.1109/LCOMM.2018.2830769.
40. Friedlander, B., Weiss, A. J. Direction finding for wideband signals using an interpolated array. *Conference Record of the Twenty-Fifth Asilomar Conference on Signals, Systems & Computers*, 1991, vol. 1, pp. 583-587 DOI: 10.1109/ACSSC.1991.186515.
41. Noureddine, L., Ferid, H., Ali, G. A joint space-time estimation algorithm for wideband signals with high resolution capabilities. *6th International Multi-Conference on Systems, Signals and Devices*, 2009, pp. 1-5. DOI: 10.1109/SSD.2009.4956659.
42. Hippenstiel, R., Fargues, M. P. Classification of wideband transient signals using spectral-based techniques. *Proceedings of 27th Asilomar Conference on Signals, Systems and Computers*, 1993, vol. 2, pp. 1479-1483. DOI: 10.1109/ACSSC.1993.342367.
43. Chernogor, L. F., Lazorenko, O. V. The modeling of ultra-wideband signals and processes. *6th International Conference on Ultrawideband and Ultrashort Impulse Signals*, 2012, pp. 246-248. DOI: 10.1109/UWBUSIS.2012.6379795.
44. Chernogor, L. F., Lazorenko, O. V., Onishchenko, A. A. New models of the fractal ultra-wideband signals. *8th International Conference on Ultrawideband and Ultrashort Impulse Signals (UWBUSIS)*, 2016, pp. 89-92. DOI: 10.1109/UWBUSIS.2016.7724158.
45. Volosyuk, V. K., Kravchenko, V. F. *Statisticheskaya teoriya radiotekhnicheskikh sistem distantsionnogo zondirovaniya i radiolokatsii* [Statistical Theory of Radio-Engineering Systems of Remote Sensing and Radar]. Moscow, Fizmatlit Publ., 2008. 704 p.
46. Volosyuk, V. K., Ksendzuk, A. V., Eskov, S. N. Optimal estimation of the radar cross-section for the stochastic surface models. *Fourth International Kharkov Symposium 'Physics and Engineering of Millimeter and Sub-Millimeter Waves'. Symposium Proceedings (Cat. No.01EX429)*, 2001, vol. 1, pp. 438-440.
47. Yanik, M. E., Torlak, M. Near-Field MIMO-SAR Millimeter-Wave Imaging With Sparsely Sampled Aperture Data. *IEEE Access*, 2019, vol. 7, pp. 31801-31819, DOI: 10.1109/ACCESS.2019.2902859.
48. Sharma, G. Raj, A. B. Spotlight SAR Imaging with Sufficient Cyclic Prefix-OFDM Waveform. *2020 International Conference on Smart Electronics and*

- Communication (ICOSEC)*, 2020, pp. 625-630, DOI: 10.1109/ICOSEC49089.2020.9215293.
49. Pavlikov, V., Volosyuk, V., Zhyla, S., Tserne, E., Shmatko, O., Sobkolov, A. Active-Passive Radar for Radar Imaging from Aerospace Carriers. *IEEE 19th International Conference on Smart Technologies (EUROCON)*, 2021, pp. 18-24. DOI: 10.1109/EUROCON52738.2021.9535619.
50. Pavlikov, V., Volosyuk, V., Zhyla, S., Sobkolov, A., Odokienko, O., Tserne, E., Shmatko, O., Sobkolov, A. Development of Broadband Criterion for Spatially Distributed Radio Systems Synthesis. *IEEE 3rd Ukrainian Conference on Electrical and Computer Engineering (UKRCON)*, 2021, pp. 232-236.
51. Kuzmenko, N. S., Ostroumov, I. V., Marais, K. An Accuracy and Availability Estimation of Aircraft Positioning by Navigational Aids. In *Proceedings of the 2018 IEEE 5th International Conference on Methods and Systems of Navigation and Motion Control (MSNMC)*, 2018, pp. 36-40. DOI: 10.1109/MSNMC.2018.8576276.
52. Sezginer, K., Güll, M., Beköz, A., Özer Y. B., Kasnakoğlu, C. DME/DME position and velocity estimation. *26th Signal Processing and Communications Applications Conference (SIU)*, 2018, pp. 1-4. DOI: 10.1109/SIU.2018.8404414.
53. Ostroumov, I. V., Kuzmenko, N. S. Compatibility analysis of multi signal processing in APNT with current navigation infrastructure. *Telecommunications and Radio Engineering*, 2018, vol. 77, no. 3, pp. 211-223. DOI: 10.1615/TelecomRadEng.v77.i3.30.
54. Zaliskyi, M., Solomentsev, O., Shcherbyna, O., Ostroumov, I., Sushchenko, O., Averyanova, Y., Heteroskedasticity Analysis During Operational Data Processing of Radio Electronic Systems. *Data Science and Security. Lecture Notes in Networks and Systems*, 2021, vol. 290. Shukla, S., Unal, A., Varghese, Kureethara J., Mishra, D. K., Han, D. S. (Eds). Singapore, Springer Publ., 2021, pp. 168-175. DOI: 10.1007/978-981-16-4486-3_18.
55. Tsymbal, O. V., Lukin, V. V., Ponomarenko, N. N. et al. Three-State Locally Adaptive Texture Preserving Filter for Radar and Optical Image Processing. *EURASIP J. Adv. Signal Process.* 851609, 2005, DOI: 10.1155/ASP.2005.1185.
56. Uss, M., Vozel, B., Lukin, V. et al. Image Informative Maps for Estimating Noise Standard Deviation and Texture Parameters. *EURASIP J. Adv. Signal Process.* 806516, 2011, DOI: 10.1155/2011/806516.

Надійшла до редакції 10.04.2021, розглянута на редколегії 23.09.2021

АЕРОКОСМІЧНИЙ БОРТОВИЙ РАДІОЛОКАЦІЙНИЙ КОМПЛЕКС ФОРМУВАННЯ ЗОБРАЖЕНЬ З РСА ТА РАС

**В. В. Павліков, К. Г. Белоусов, С. С. Жила, Е. О. Церне, О. О. Шматко, А. Д. Собколов,
Д. С. Власенко, В. В. Кошарський, О. В. Одокіенко, М. В. Руженцев**

Предметом вивчення в статті є алгоритми радіомоніторингу Землі у широкій зоні огляду з аерокосмічного транспорту. Метою є розробка структурної схеми радіокомплексу, який може працювати одночасно у двох режимах: модифікованого синтезування апертури антени (РСА) і апертурного синтезу (РАС), відповідно до алгоритмів, синтезованих методом максимальної правдоподібності. Режим модифікованого РСА дозволяє отримати радіозображення високого розрізnenня у діапазоні кутів спостереження $\pm(20^\circ \dots 50^\circ)$ від напрямку в надир. Використовується метод поєднання модифікованого алгоритму РСА, який відрізняється від класичного алгоритму формування зображення можливістю отримання більш високої просторової роздільної здатності, платою за це є ускладнення алгоритму обробки сигналів, пов'язане з реалізацією декоррелюючих фільтрів, які розширяють спектр прийнятих сигналів в кожному приймальному тракті, та режиму РАС, який дозволяє формувати зображення за допомогою принципів пасивної або активної радіолокації. Пасивний режим РАС передбачає побудову зображення у діапазоні кутів спостереження $\pm 20^\circ$ від надиру за результатами оброблення сигналів власного широкосмугового радіотеплового випромінювання, а активний – у цьому ж діапазоні кутів спостереження але з використанням широкосмугового шумового сигналу підсвічування. Важливим результатом у формуванні радіозображення у зазначеній зоні огляду при використанні активного режиму роботи РАС є те, що зображення є близькими за фізичним змістом, а саме пропорційні питомій ефективній поверхні відбиття підстильної поверхні. Крім того, відмінною рисою синтезованих алгоритмів є використання широкосмугових зондуючих сигналів і, відповідно, таких же вхідних трактів приймачів, що дозволяє підвищити відношення сигнал/шум вихідного ефекту. Висновки. Наукова новизна отриманих результатів полягає в наступному: було розроблено структурну схему радіокомплексу на основі алгоритмів, синтезованих методом максимальної правдоподібності. Для формування радіозображення в радіокомплексі реалізовано поєднання РСА і РАС (з двома режимами роботи). Дані реалізація має важливе значення, адже дозволяє отримувати зображення високої розрізнювальної здатності у діапазоні кутів спостереження $\pm 50^\circ$.

від напрямку у надир. Комплекс доцільно розміщувати на літаках, вертолютах і космічних апаратах (бажано тих, які рухаються по низьким орбітам).

Ключові слова: формування радіозображеній; радар з синтезом апертури; радар з апертурним синтезом; алгоритм обробки сигналу; обробка надширокосмугового сигналу.

АЭРОКОСМИЧЕСКИЙ БОРТОВОЙ РАДИОЛОКАЦИОННЫЙ КОМПЛЕКС ФОРМИРОВАНИЯ ИЗОБРАЖЕНИЙ С РСА И РАС

*В. В. Павликov, К. Г. Белоусов, С. С. Жила, Э. А. Цернэ, А. А. Шматко, А. Д. Собковов,
Д. С. Власенко, В. В. Кошарский, А. В. Одокиенко, Н. В. Руженцев*

Предметом изучения в статье являются алгоритмы радиомониторинга Земли в широкой зоне обзора с аэрокосмического транспорта. Целью является разработка структурной схемы радиокомплекса, который может работать одновременно в двух режимах: модифицированного синтезирования апертуры антенны (РСА) и апертурного синтеза (РАС), в соответствии с алгоритмами, синтезированными методом максимального правдоподобия. Режим модифицированного РСА позволяет получить радиоизображения высокого разрешения в диапазоне углов наблюдения $\pm(20^\circ...50^\circ)$ от направления в надир. Используется метод сочетания модифицированного алгоритма РСА, который отличается от классического алгоритма формирования изображения возможностью получения более высокого пространственного разрешения, платой за это является усложнение алгоритма обработки сигналов, связанное с реализацией декоррелирующих фильтров, которые расширяют спектр принимаемых сигналов в каждом приемном тракте, и режима РАС, который позволяет формировать изображение с помощью принципов пассивной или активной радиолокации. Пассивный режим РАС предусматривает построение изображения в диапазоне углов наблюдения $\pm 20^\circ$ от надира по результатам обработки сигналов собственного широкополосного радиотеплового излучения, а активный – в этом же диапазоне углов наблюдения, но с использованием широкополосного шумового сигнала подсветки. Важным результатом в формировании радиоизображения в указанной зоне обзора при использовании активного режима работы РАС является то, что изображения близки по физическому содержанию, а именно пропорциональны удельной эффективной поверхности отражения подстилающей поверхности. Кроме того, отличительной чертой синтезированных алгоритмов является использование широкополосных зондирующих сигналов и, соответственно, таких же входных трактов приемников, что позволяет повысить отношение сигнал / шум выходного эффекта. Выводы. Научная новизна полученных результатов заключается в следующем: была разработана структурная схема радиокомплекса на основе алгоритмов, синтезированных методом максимального правдоподобия. Для формирования радиоизображения в радиокомплексе реализовано сочетание РСА и РАС (с двумя режимами работы). Данная реализация имеет важное значение, поскольку позволяет получать изображения высокой разрешающей способности в диапазоне углов наблюдения $\pm 50^\circ$ от направления в надир. Комплекс целесообразно размещать на самолетах, вертолетах и космических аппаратах (желательно тех, которые движутся по низким орбитам).

Ключевые слова: формирование радиоизображений; радар с синтезом апертуры; радар с апертурным синтезом; алгоритм обработки сигнала; обработка сверхширокополосного сигнала.

Павліков Володимир Володимирович – д-р техн. наук, старш. наук. співроб., проректор з наукової роботи, Національний аерокосмічний університет ім. М. Є. Жуковського «Харківський авіаційний інститут», Харків, Україна.

Белоусов Костянтин Георгійович – головний конструктор і начальник проектно-конструкторського бюро космічних апаратів, систем вимірювань і телекомунікацій КБ Південне, Дніпро, Україна.

Жила Семен Сергійович – д-р техн. наук, зав. каф. аерокосмічних радіоелектронних систем, Національний аерокосмічний університет ім. М. Є. Жуковського «Харківський авіаційний інститут», Харків, Україна.

Цернє Едуард Олексійович – асист. каф. аерокосмічних радіоелектронних систем, Національний аерокосмічний університет ім. М. Є. Жуковського «Харківський авіаційний інститут», Харків, Україна.

Шматко Олександр Олександрович – канд. техн. наук, докторант каф. аерокосмічних радіоелектронних систем, Національний аерокосмічний університет ім. М. Є. Жуковського «Харківський авіаційний інститут», Харків, Україна.

Собковов Антон Дмитрович – наук. співроб. каф. аерокосмічних радіоелектронних систем, Національний аерокосмічний університет ім. М. Є. Жуковського «Харківський авіаційний інститут», Харків, Україна.

Власенко Дмитро Сергійович – асист. каф. аерокосмічних радіоелектронних систем, Національний аерокосмічний університет ім. М. Є. Жуковського «Харківський авіаційний інститут», Харків, Україна.

Кошарський Володимир Віталійович – асист. каф. аерокосмічних радіоелектронних систем, Національний аерокосмічний університет ім. М. Є. Жуковського «Харківський авіаційний інститут», Харків, Україна.

Одокієнко Олексій Володимирович – канд. техн. наук, декан факультету радіоелектронних комп’ютерних систем та інфокомунікацій, Національний аерокосмічний університет ім. М. Є. Жуковського «Харківський авіаційний інститут», Харків, Україна.

Руженцев Микола Васильович – д-р техн. наук, проф., головн. наук. співроб. каф. аерокосмічних радіоелектронних систем, Національний аерокосмічний університет ім. М. Є. Жуковського «Харківський авіаційний інститут», Харків, Україна.

Volodimir Pavlikov – D.Sc. in Radioengineering, Vice rector for Science, National Aerospace University "Kharkiv Aviation Institute", Kharkiv, Ukraine,
e-mail: v.pavlikov@khai.edu, ORCID: 0000-0002-6370-1758.

Konstantin Belousov – Chief Designer, Head of Spacecraft, Measuring Systems and Telecommunications in Yuzhnole SDO, Dnipro, Ukraine,
ORCID: 0000-0002-6436-3359.

Simeon Zhyla – D.Sc. in Radioengineering, Head of Department of Aerospace Radio-electronic Systems, National Aerospace University "Kharkiv Aviation Institute", Kharkiv, Ukraine,
e-mail: s.zhyla@khai.edu, ORCID: 0000-0003-2989-8988.

Eduard Tserne – Assistant of Department of Aerospace Radio-electronic Systems, National Aerospace University "Kharkiv Aviation Institute", Kharkiv, Ukraine,
e-mail: e.tserne@khai.edu, ORCID: 0000-0003-0709-2238.

Olexandr Shmatko – PhD in Radioengineering, doctoral student of Department of Aerospace Radio-electronic Systems, National Aerospace University "Kharkiv Aviation Institute", Kharkiv, Ukraine,
e-mail: o.shmatko@khai.edu, ORCID: 0000-0002-3236-0735.

Anton Sobkolov – Researcher of Department of Aerospace Radio-electronic Systems, National Aerospace University "Kharkiv Aviation Institute", Kharkiv, Ukraine,
e-mail: a.sobkolov@khai.edu, ORCID: 0000-0001-9356-4187.

Dmytro Vlasenko – Assistant of Department of Aerospace Radio-electronic Systems, National Aerospace University "Kharkiv Aviation Institute", Kharkiv, Ukraine,
e-mail: d.vlasenko@khai.edu, ORCID: 0000-0002-6118-2173.

Volodimir Kosharskyi – Assistant of Department of Aerospace Radio-electronic Systems, National Aerospace University "Kharkiv Aviation Institute", Kharkiv, Ukraine,
e-mail: v.kosharsky@khai.edu, ORCID: 0000-0002-8569-2047.

Olexiy Odokiienko – PhD in Radioengineering, National Aerospace University "Kharkiv Aviation Institute", Kharkiv, Ukraine,
e-mail: o.odokiienko@khai.edu, ORCID: 0000-0002-5227-1000.

Mykola Ruzhentsev – D.Sc., Professor, Chief Research Fellow of Department of Aerospace Radio-electronic Systems, National Aerospace University "Kharkiv Aviation Institute", Kharkiv, Ukraine,
e-mail: m.ruzhentsev@khai.edu, ORCID: 0000-0003-3023-4927.